Chemical Engineering Journal 141 (2008) 387–392

Contents lists available at ScienceDirect

Chemical Engineering Journal

journal homepage: www.elsevier.com/locate/cej

Short communication

Effect of dispersed phase rheology on the drag of single and of ensembles of fluid spheres at moderate Reynolds numbers

N. Kishore [a], R.P. Chhabra [a,*], V. Eswaran [b]

[a] Department of Chemical Engineering, Indian Institute of Technology, Kanpur 208016, India
[b] Department of Mechanical Engineering, Indian Institute of Technology, Kanpur 208016, India

ARTICLE INFO

Article history:
Received 21 September 2007
Received in revised form 26 January 2008
Accepted 27 March 2008

Keywords:
Fluid sphere
Viscous drop
Drag
Power-law liquids
Rheology

ABSTRACT

In this work, the effect of dispersed phase rheology on the drag phenomena of single and of ensembles of fluid spheres translating in an immiscible power-law continuous phase has been studied numerically at moderate Reynolds numbers. The results presented herein encompass the following ranges of conditions: $1 \le Re_o \le 200$, $0.1 \le k \le 50$, $0.2 \le \Phi \le 0.6$, $0.6 \le n_i \le 1.6$ and $0.6 \le n_o \le 1.6$, thereby enabling the effects of the Reynolds number (Re_o), of the internal to external fluid characteristic viscosity ratio (k), of the volume fraction of the dispersed phase (Φ) and of the two power-law indices (n_i, n_o) on drag coefficient to be delineated. This information facilitates the estimation of the rate of sedimentation of single fluid spheres and their ensembles in quiescent continuous phase. Within the range of conditions studied herein, the effect of the dispersed phase rheology is found to be rather small.

1. Introduction

Due to their wide ranging applications in chemical, biological and processing industries, considerable effort has been devoted to the study of the hydrodynamic behaviour of fluid spheres in another immiscible liquid phase [1,2]. While numerous studies dealing with the behaviour of single particles provide useful insights, one frequently encounters ensembles of droplets in engineering applications. In recent years, considerable research efforts have been directed in developing reliable theoretical/numerical methods for the prediction of the settling velocity in liquid–liquid systems to evaluate their stability and/or to estimate the available contact time between the two phases. Over the years, significant information has been reported on the settling velocity of single fluid spheres [3–5] and their ensembles [6–8]. Thus, it is possible to estimate the settling velocity of the dispersed phase in these systems over conditions of practical interest when both phases are Newtonian fluids.

On the other hand, many high molecular weight polymers and their solutions, slurries, foams and emulsions encountered in several industrially important applications display shear-thinning, shear-thickening, yield stress and viscoelastic behaviour [9]. Due to the wide occurrence of non-Newtonian fluid behaviour, many studies are available which elucidate the influence of the continuous phase rheology (especially of shear-thinning and viscoelasticity) on the drag of single Newtonian fluid spheres, e.g., see Refs. [10–14] and for ensembles of fluid spheres [15–18]. Hence, reliable drag results are now available over the ranges of conditions ($1 \le Re_o \le 200$, $0.6 \le n_o \le 1.6$, $0.1 \le k \le 50$) for single spheres and over the range of volume fraction of the dispersed phase ($0.2 \le \Phi \le 0.6$) for ensembles. Broadly speaking, shear-thinning fluid behaviour reduces drag while shear-thickening enhances it as compared to its value in Newtonian continuous media otherwise under identical conditions.

In contrast, very little is known about the case when the dispersed phase or both phases exhibit non-Newtonian behaviour. For instance, Tripathi and Chhabra [19] used the velocity and stress variational principles to obtain approximate upper and lower bounds on the drag of a power-law fluid sphere falling in another power-law medium. The two bounds diverge with the increasing degree of shear-thinning behaviour, i.e., the decreasing value of the power-law index. Subsequently, this work was extended to obtain approximate upper and lower bounds on the drag (or rate of sedimentation) of ensembles of fluid spheres via the free surface cell model [20]. In the creeping flow region, both these studies suggested the influence of the dispersed phase rheology to be rather small in the limit of the zero Reynolds number. On the other hand, Gurkan [21] considered the case of a power-law drop falling in a

* Corresponding author. Tel.: +91 512 2597393; fax: +91 512 2590104.
E-mail address: chhabra@iitk.ac.in (R.P. Chhabra).

1385-8947/$ – see front matter © 2008 Elsevier B.V. All rights reserved.
doi:10.1016/j.cej.2008.03.015

Newtonian continuous phase. Their results embracing the range of conditions ($10 \le Re_o \le 50$, $0.1 \le k \le 1000$ and $0.6 \le n_i \le 1$) also suggest the effect of the dispersed phase rheology to be rather small, albeit their numerical results are believe be inaccurate in the limiting case of both phases being Newtonian fluids thereby casting some doubts about the reliability of their results for power-law fluids [3–5,13].

Similarly, there have been a few experimental results involving non-Newtonian fluid spheres settling in a Newtonian continuous medium. Marrucci et al. [22] reported experimental terminal velocity data in the creeping flow regime extending over the range of parameters $0.0045 \le k \le 1.88$ and $0.53 \le n_i \le 0.745$. However, due to the contamination by surface active agents which tend to immobilize the free surface of drops, their results are in complete agreement with the Stokes expression for solid spheres, even though the highest value of the viscosity ratio, k, in their study is only of the order of 2. Gillapsy and Hoffer [23] reported experiments on the drag coefficients of Newtonian and power-law liquid drops falling in air at large Reynolds numbers and reported no difference between the drag values for Newtonian and non-Newtonian liquid drops. This is also not at all surprising as their results relate to high values of the Reynolds number wherein the role of viscosity is expected to be small. Rodrigue and Blanchet [11] and Rodrigue [14] have carried out experimental studies on the motion and shapes of viscoelastic drops in another Newtonian and/or viscoelastic fluid with or without the presence of surfactants. However, the major thrust of their study was on shape transitions and thus no drag results were reported. Also, their experimental fluids exhibited both shear-thinning and viscoelastic characteristics and therefore, it is not possible to delineate the influence of these two characteristics.

It is thus clear that no prior results are available on the drag of single fluid spheres and their ensembles when the dispersed phase or both phases exhibit power-law fluid behaviour in the moderate Reynolds number range. This work aims to fill this gap in the literature.

2. Problem statement and description

Since extensive descriptions of the problems considered herein are available elsewhere [7,13,18], only the salient features are repeated here. A spherical coordinate system (r, θ, ϕ) with its origin at the centre of the drop is used with polar axis ($\theta = 0$) directed along the direction of flow. The flow is axisymmetric, i.e., v_ϕ is zero and no flow variable depends on the ϕ-coordinate. The dimensionless governing equations for this flow in their conservative form are:

- Continuity equation

$$\frac{1}{r^2}\frac{\partial}{\partial r}[r^2(v_r)_{i,o}] + \frac{1}{r\sin\theta}\frac{\partial}{\partial\theta}[(v_\theta)_{i,o}\sin\theta] = 0 \tag{1}$$

- r-component of momentum equation

$$\frac{\partial(v_r)_{i,o}}{\partial t} + \frac{1}{r^2}\frac{\partial}{\partial r}[r^2(v_r)^2_{i,o}] + \frac{1}{r\sin\theta}\frac{\partial}{\partial\theta}[(v_r)_{i,o}(v_\theta)_{i,o}\sin\theta] - \frac{(v_\theta)^2_{i,o}}{r} = -\frac{\partial p_{i,o}}{\partial r} + \frac{2^{(n_{i,o}+1)}}{Re_{i,o}}\left[(\varepsilon_{rr})_{i,o}\frac{\partial\eta_{i,o}}{\partial r} + \frac{(\varepsilon_{r\theta})_{i,o}}{r}\frac{\partial\eta_{i,o}}{\partial\theta}\right] + \frac{2^{n_{i,o}}\eta_{i,o}}{Re_{i,o}}\left[\frac{1}{r^2}\frac{\partial^2}{\partial r^2}(r^2(v_r)_{i,o}) + \frac{1}{r^2\sin\theta}\frac{\partial}{\partial\theta}\left(\sin\theta\frac{\partial(v_r)_{i,o}}{\partial\theta}\right)\right] \tag{2}$$

- θ-component of momentum equation

$$\frac{\partial(v_\theta)_{i,o}}{\partial t} + \frac{1}{r^2}\frac{\partial}{\partial r}[r^2(v_r)_{i,o}(v_\theta)_{i,o}] + \frac{1}{r\sin\theta}\frac{\partial}{\partial\theta}[(v_\theta)^2_{i,o}\sin\theta] + \frac{(v_r)_{i,o}(v_\theta)_{i,o}}{r} = -\frac{1}{r}\frac{\partial p_{i,o}}{\partial\theta} + \frac{2^{(n_{i,o}+1)}}{Re_{i,o}}\left[(\varepsilon_{r\theta})_{i,o}\frac{\partial\eta_{i,o}}{\partial r} + \frac{(\varepsilon_{\theta\theta})_{i,o}}{r}\frac{\partial\eta_{i,o}}{\partial\theta}\right] + \frac{2^{n_{i,o}}\eta_{i,o}}{Re_{i,o}}\left[\frac{1}{r^2}\frac{\partial}{\partial r}\left(r^2\frac{\partial(v_\theta)_{i,o}}{\partial r}\right) + \frac{1}{r^2}\frac{\partial}{\partial\theta}\left(\frac{1}{\sin\theta}\frac{\partial}{\partial\theta}[(v_\theta)_{i,o}\sin\theta]\right) + \frac{2}{r^2}\frac{\partial(v_r)_{i,o}}{\partial\theta}\right] \tag{3}$$

where subscripts i, o represent the internal (dispersed phase) and the external (continuous phase) flow variables, respectively. For an incompressible fluid, the extra stress tensor (τ_{xy}) is related to the rate of strain tensor (ε_{xy}) as:

$$\tau_{xy} = 2\eta\varepsilon_{xy}; \quad x,\ y = r,\ \theta,\ \phi \tag{4}$$

The viscosity of a power-law liquid is given as:

$$\eta = \left(\frac{\prod_\varepsilon}{2}\right)^{(n-1)/2} \tag{5}$$

where $\prod_\varepsilon$ is the second invariant of the rate of deformation tensor and its expression in terms of v_r and v_θ and their derivatives is available in standard books (e.g., see [24]). Eq. (5) represents shear-thinning, Newtonian and shear-thickening fluid behaviour for $n < 1$, $n = 1$ and $n > 1$, respectively. In the above equations, velocity has been scaled using U_o, radial coordinate using the drop radius R, pressure using ρU_o^2, components of the rate of strain tensor by U_o/R, viscosity by a reference viscosity η_{ref} (=m$(U_o/R)^{(n-1)}$), extra stress components by $\eta_{ref}(U_o/R)$ and time by R/U_o. Here m is the power-law fluid consistency index and n is the power-law behaviour index. The Reynolds number for the external phase is defined as follows:

$$Re_o = \frac{\rho_o U_o^{(2-n_o)}(2R)^{n_o}}{m_o} \tag{6}$$

The two Reynolds numbers, Re_i and Re_o are inter-related via the characteristic viscosity ratio and the density ratio as follows:

$$Re_i = \frac{Re_o\lambda}{k} \tag{7}$$

where ρ is the density of fluid, λ is the density ratio (ρ_i/ρ_o) and k is the characteristic viscosity ratio defined as:

$$k = \left(\frac{m_i}{m_o}\right)\left(\frac{2R}{U_o}\right)^{(n_o-n_i)} \tag{8}$$

For treating the motion of ensembles, within the framework of the free surface cell model [25], the inter-drop interactions are approximated by postulating each drop to be surrounded by a hypothetical envelope of the continuous fluid of radius R_∞ [1,7,8,15–18,25]. The dimensionless radius of the outer spherical envelope is related to the overall mean volume fraction of the dispersed phase, Φ, as:

$$R_\infty = \Phi^{-1/3} \tag{9}$$

Therefore, by simply varying the value of R_∞, one can simulate the ensembles of different volume fractions of the dispersed phase including the limiting case of a single droplet by setting $R_\infty \to \infty$, i.e., $\Phi \to 0$.

The relevant boundary conditions for this flow can be written in their dimensionless form as follows:

- At the outer boundary ($r = R_\infty$):

$$(v_r)_o = -\cos\theta \tag{10}$$

$$(v_\theta)_o = \sin\theta; \quad \text{for the case of a single drop} \tag{11}$$

$$(\tau_{r\theta})_o = 0; \quad \text{for the case of an ensemble of drops} \tag{12}$$

- At the fluid–fluid interface ($r = 1$):

$$(v_r)_i = (v_r)_o = 0 \tag{13}$$

$$(v_\theta)_i = (v_\theta)_o \tag{14}$$

$$(\tau_{r\theta})_i = (\tau_{r\theta})_o \tag{15}$$

- Along the axis of symmetry ($\theta = 0,\pi$):

$$(v_\theta)_i = 0; \quad \frac{\partial (v_r)_i}{\partial \theta} = 0 \tag{16}$$

$$(v_\theta)_o = 0; \quad \frac{\partial (v_r)_o}{\partial \theta} = 0 \tag{17}$$

- At the centre of the drop ($r = 0$):

$$(v_r)_i \text{ and } (v_\theta)_i \text{ remain finite} \tag{18}$$

Once the fully converged velocity and pressure fields are known, the individual and total drag coefficients can be evaluated using the following expressions:

$$C_d = \frac{2F_d}{\rho_o U_o^2 \pi R^2} = C_{dp} + C_{df} \tag{19}$$

where the pressure and frictional components of the total drag, C_{dp} and C_{df}, respectively, can be expressed as follows:

$$C_{dp} = 2\int_o^\pi [p_o \sin 2\theta]_{r=1}\, d\theta \tag{20}$$

$$C_{df} = \frac{2^{(n_o+2)}}{Re_o}\int_0^\pi \left\{ \eta_o \left[\left(\frac{\partial (v_\theta)_o}{\partial r} - \frac{(v_\theta)_o}{r} \right) \sin^2\theta - \left(\frac{\partial (v_r)_o}{\partial r} \right) \sin 2\theta \right] \right\}_{r=1} d\theta \tag{21}$$

3. Numerical methodology

3.1. Numerical details

Since detailed descriptions of the numerical solution method used herein are available elsewhere [7,13,18], only salient features are presented here. The governing Eqs. (1–3), subject to the boundary conditions outlined in Eqs. (10–18) have been solved by a finite difference method based SMAC-implicit algorithm implemented on a staggered grid arrangement. This is a simplified version of the MAC method due to Harlow and Welch [26] which has been adapted for power-law fluids. The diffusive and non-Newtonian terms in the momentum equation have been discretized using a second order central differencing scheme, whereas the convective terms were discretized using the QUICK scheme [27].

3.2. Grid independence

In this study, the case of a single fluid sphere was simulated by setting the radius of the outer fluid envelope to be 150, i.e., $R_\infty = 150$ [13]; whereas, in the case of ensembles of fluid spheres, the value of the dispersed phase concentration was varied over the range of $0.2 \le \Phi \le 0.6$ which corresponds to $1.186 \le R_\infty \le 1.71$ [7,18]. Furthermore, in the case of a single fluid sphere, a fine grid in the vicinity of the drop was obtained by using a logarithmic stretching ($y = \ln r$), as has been done by many others [3–5] and in our recent study [13]. In the case of a single power-law fluid sphere, extensive grid independence was carried at $Re_o = 500$ and for the extreme values of viscosity ratio and of the two power-law indices (see Table 1). It can be seen from this table, that the three grids produce results which are within ±2–3% of each other. Thus, bearing in mind an optimum CPU time, the second grid of size 90×240 has been used in the present study for single fluid spheres. Similarly, Table 2 shows the effect of grid size in the case of multiple fluid spheres of hold-up, $\Phi = 0.2$. Once again, the three grids tested here produce nearly identical results. Thus, a grid of size 60×70 ($3^\circ \times 0.025$) has been used in this study for all values of Re_o, k, n_i, n_o and Φ. Finally, it should be noted that the optimum grids found herein are identical to that used in our previous studies dealing with the Newtonian dispersed phase [7,13,18].

Table 1
Effect of grid size on the value of drag coefficient of a single power-law fluid sphere at $Re_o = 500$

Grid ($\theta \times r$)	$k = 0.1$		$k = 10$	
	$n_i = n_o = 0.6$	$n_i = n_o = 1.6$	$n_i = n_o = 0.6$	$n_i = n_o = 1.6$
60×240	0.0591	0.1921	0.2853	0.8251
90×240	0.0584	0.1935	0.2848	0.8339
90×300	0.0604	0.1914	0.2838	0.8434

Table 2
Effect of grid size on the value of drag coefficient of multiple power-law fluid spheres ($\Phi = 0.2$ and $Re_o = 200$)

Grid ($\theta \times r$)	$k = 0.1$		$k = 10$	
	$n_i = n_o = 0.6$	$n_i = n_o = 1.6$	$n_i = n_o = 0.6$	$n_i = n_o = 1.6$
45×70	0.2598	0.8460	1.0598	3.8771
60×70	0.2638	0.8511	1.0560	3.8785
60×85	0.2627	0.8407	1.0786	3.8325

4. Results and discussion

4.1. Validation of results

The extensive benchmarking and validation for the flow of Newtonian and power-law fluids over a single and clusters of fluid (Newtonian) and rigid spheres have been reported elsewhere [7,13,18]. Table 3 shows the additional comparisons of C_d for ensembles of fluid spheres in creeping flow regime when both phases display power-law behaviour with the results of Tripathi and Chhabra [20]. The present results are in good agreement only for a mild degree of shear-thinning behaviour and the correspondence between the two deteriorates rapidly with the increasing degree of shear-thinning and/or the value of k. However, it should be noted here that the two bounds are not only approximate, but also coincide only for Newtonian fluids and indeed these diverge from each other increasingly with the decreasing value of the power-law index. Therefore, the present results are expected to be more reliable than the approximate results [20]. Bearing in mind these factors coupled with our previous experience [7,13,18], the present results are believed to be accurate to within ±2–4%.

Table 3
Comparison of C_d of ensembles ($\Phi = 0.2$) at $Re_o = 1$

k	$n_i = n_o = 0.8$		$n_i = n_o = 0.6$	
	Tripathi and Chhabra [20]	Present	Tripathi and Chhabra [20]	Present
0.1	32.904	33.2730	25.212	26.6907
1	53.460	51.7383	40.810	38.3104
10	86.570	83.9262	61.740	54.0619

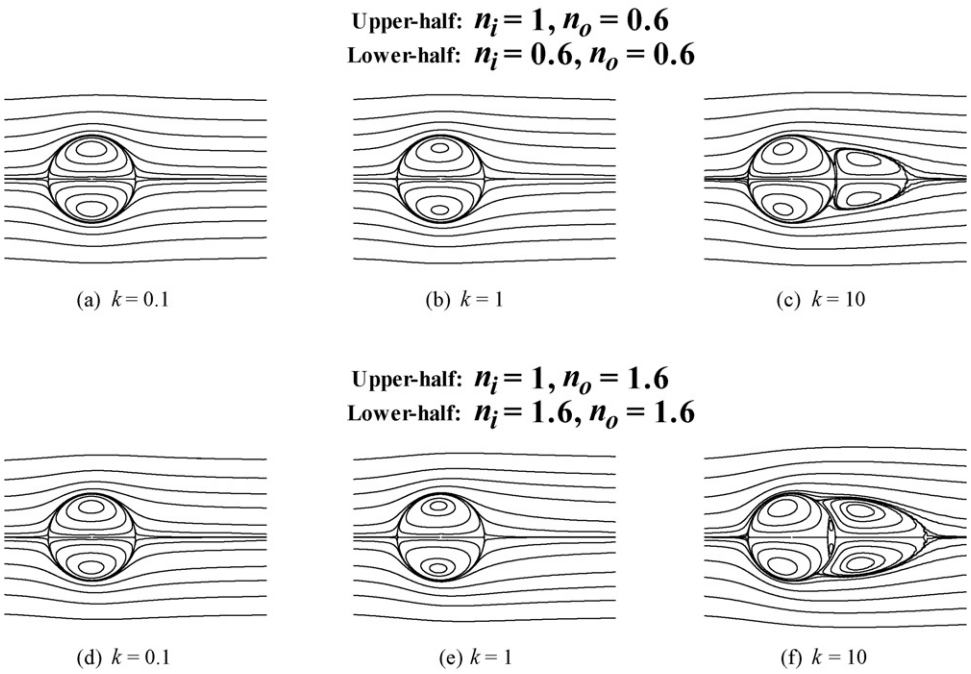

Fig. 1. Representative streamline patterns of power-law fluid flow over a single Newtonian (upper-half) and a power-law (lower-half) fluid sphere at $Re_o = 200$ for different values of k.

4.2. Flow patterns

Fig. 1(a–c) shows the streamline patterns for a shear-thinning fluid ($n_o = 0.6$) flowing over a Newtonian fluid sphere, $n_i = 1$ (upper-half) and over a shear-thinning fluid sphere, $n_i = 0.6$ (lower-half) at $Re_o = 200$ for different values of k. In the upper-half (Newtonian fluid sphere), for $k \leq 1$, the streamlines in the external phase exhibit fore and aft symmetry; also, the centres of the internal circulations

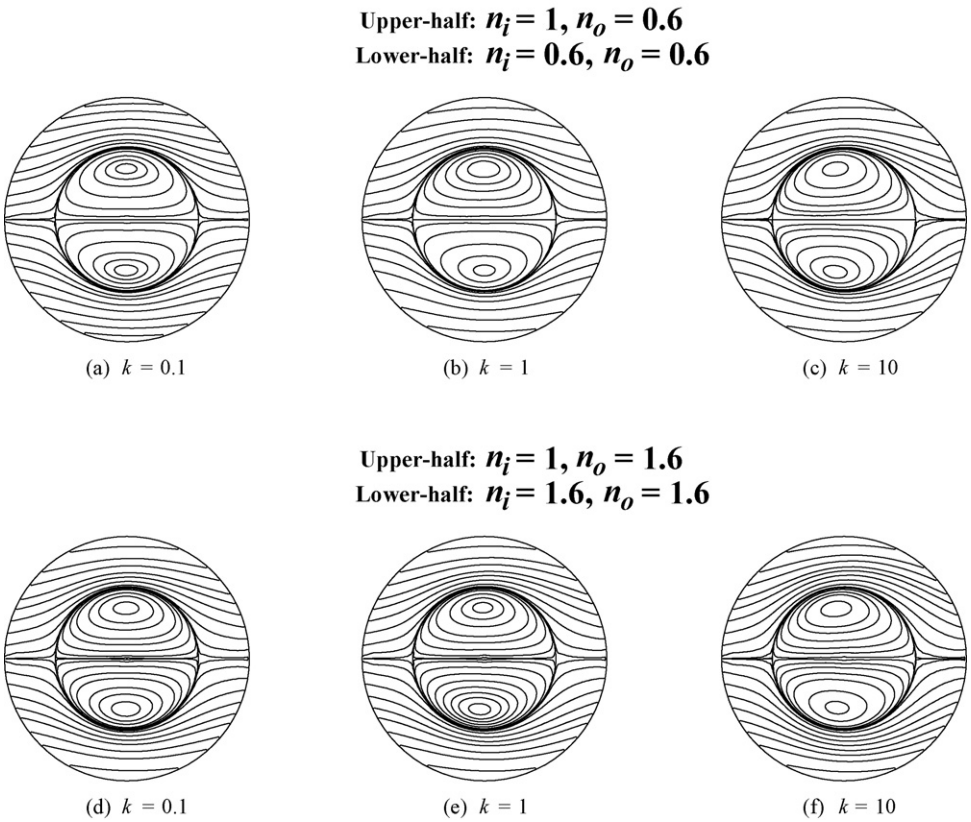

Fig. 2. Representative streamline patterns for power-law fluid flow in ensembles of Newtonian (upper-half) and of power-law (lower-half) fluid spheres for $\Phi = 0.2$ at $Re_o = 200$ for different values of k.

and of the drop are in the same line which is perpendicular to the horizontal axis thereby showing a perfect symmetry of the internal flow as that in the external phase. For $k = 10$, a non-contiguous wake is formed in the rear end of the drop which is obviously not due to the flow separation, as the interfacial angular velocity does not become zero in this case. Also for $k = 10$, the centre of the internal circulation moves towards the front stagnation point of the drop which suggests the presence of excess vorticity which, in turn, produces a non-contiguous wake without flow separation. Similar trends can be seen in the lower-half (shear-thinning fluid sphere, $n_i = 0.6$ in a shear-thinning fluid, $n_o = 0.6$) for different values of k. Fig. 1(d–f) shows the streamline patterns for a shear-thickening fluid ($n_o = 1.6$) flowing past a Newtonian fluid sphere, $n_i = 1$ (upper-half) and a shear-thickening fluid sphere, $n_i = 1.6$ (lower-half) at $Re_o = 200$ for different values of k. Once again, in the upper-half (Newtonian fluid sphere), similar trends are observed for $k \leq 1$ as in the case of a shear-thinning ($n_o = 0.6$) continuous phase. But for $k = 10$, the non-contiguous wake is attached to the surface of the drop and also a significant increase in the size of the wake has been observed. In the lower-half (shear-thickening fluid sphere, $n_i = 1.6$), similar trends can be seen as in the case of a Newtonian fluid sphere (upper-half) in a shear-thickening fluid, $n_o = 1.6$. Qualitatively similar trends observed for other values of Re_o, n_i, n_o and k and thus these are not shown here.

Fig. 2(a–c) shows typical streamline patterns of a shear-thinning fluid ($n_o = 0.6$) in ensembles of Newtonian fluid spheres, $n_i = 1$ (upper-half) and of shear-thinning fluid spheres, $n_i = 0.6$ (lower-half) of $\Phi = 0.2$ at $Re_o = 200$ for different values of k. Both upper and lower halves appear to be mirror image of each other. Similar observations can be made from Fig. 2(d–f), where the dispersed phase is changed from Newtonian ($n_i = 1$) to a shear-thickening fluid ($n_i = 1.6$) by keeping the continuous phase fixed as a shear-thickening fluid ($n_o = 1.6$). Thus, it is clear that even in the case of ensembles of fluid spheres, the droplet phase rheology has very little effect on the external flow field.

4.3. Drag phenomena

Table 4 shows the effect of Re_o and k on the drag of a single shear-thinning ($n_i = 0.6$) fluid sphere in a Newtonian continuous medium ($n_o = 1$). This dependence is seen to be qualitatively similar as that reported when the dispersed phase is Newtonian fluid [3–5,13]. This table also shows the effect of the dispersed phase rheology. The ratio between the drag of a power-law drop ($n_i \neq 1$) to that of a Newtonian drop ($n_i = 1$) in an another immiscible power-law liquid

Table 4
Drag on a power-law fluid sphere in a Newtonian fluid

Re_o	k	C_d	$C_d\ (n_i \neq 1)/C_d\ (n_i = 1)$
$n_i = 0.6, n_o = 1$			
200	0.1	0.2216	0.9982
	10	0.7792	1.0539
5	0.1	4.5010	1.0046
	10	7.2538	1.0316
$n_i = 1, n_o = 0.6$			
200	0.1	0.1495	–
	10	0.4274	–
5	0.1	0.8859	–
	10	4.7657	–
$n_i = 1.6, n_o = 1$			
200	0.1	0.2363	1.0644
	10	0.7409	1.0022
5	0.1	4.4736	0.9985
	10	7.1589	1.0182
$n_i = 1, n_o = 1.6$			
200	0.1	0.3966	–
	10	1.2064	–
1	0.1	4.2611	–
	10	6.5583	–

Table 5
Drag on a power-law fluid sphere in a power-law fluid

Re_o	k	C_d	$C_d\ (n_i = n_o)/C_d\ (n_i = 1 \neq n_o)$
$n_i = n_o = 0.6$			
200	0.1	0.1454	0.9726
	10	0.4306	1.0075
5	0.1	0.8823	0.9959
	10	4.9484	1.0383
$n_i = n_o = 1.6$			
200	0.1	0.4001	1.0088
	10	1.1923	0.9883
5	0.1	4.2269	0.9919
	10	6.5251	0.9949

Table 6
Drag on ensembles of power-law fluid spheres in a Newtonian fluid

Φ	Re_o	k	C_d	$C_d\ (n_i \neq 1)/C_d\ (n_i = 1)$
$n_i = 0.6, n_o = 1$				
0.2	200	0.1	0.4340	0.9857
		10	2.0163	1.0084
	1	0.1	42.4236	1.0075
		10	122.9937	1.0045
$n_i = 1, n_o = 0.6$				
	200	0.1	0.2832	–
		10	1.0387	–
	1	0.1	26.3009	–
		10	58.3511	–
$n_i = 1.6, n_o = 1$				
	200	0.1	0.4392	0.9982
		10	1.9547	0.9778
	1	0.1	42.6171	1.0121
		10	120.1012	0.9891
$n_i = 1, n_o = 1.6$				
	200	0.1	0.8283	–
		10	3.9286	–
	1	0.1	91.6090	–
		10	362.4823	–
$n_i = 0.6, n_o = 1$				
0.6	200	0.1	1.1033	0.9707
		10	11.6267	0.9906
	1	0.1	128.4827	1.0043
		10	1433.9419	1.0250
$n_i = 1, n_o = 0.6$				
	200	0.1	0.6296	–
		10	3.5175	–
	1	0.1	50.0230	–
		10	293.1670	–
$n_i = 1.6, n_o = 1$				
	200	0.1	1.1549	1.0166
		10	11.5123	0.9809
	1	0.1	125.9681	0.9831
		10	1369.9318	0.9793
$n_i = 1, n_o = 1.6$				
	200	0.1	3.139	–
		10	72.221	–
	1	0.1	574.436	–
		10	14180.24	–

Table 7
Drag on ensembles of power-law fluid spheres in a power-law fluid

Φ	Re_o	k	C_d	$C_d\ (n_i \neq 1)/C_d\ (n_i = 1)$
$n_i = n_o = 0.6$				
0.2	200	0.1	0.2638	0.9315
		10	1.0560	1.0166
	1	0.1	26.6907	1.0148
		10	54.0619	0.9265
$n_i = n_o = 1.6$				
	200	0.1	0.8511	1.0275
		10	3.8785	0.9872
	1	0.1	92.3919	1.0085
		10	374.069	1.0320
$n_i = n_o = 0.6$				
0.6	200	0.1	0.5995	0.9522
		10	3.8335	1.0898
	1	0.1	50.4087	1.0077
		10	289.680	0.9881
$n_i = n_o = 1.6$				
	200	0.1	3.1943	1.0176
		10	69.8780	0.9676
	1	0.1	568.1614	0.9891
		10	13554.15	0.9558

is seen to be almost unity thereby implying the negligible effect of the dispersed phase rheology for both shear-thinning and shear-thickening drops under otherwise identical conditions. Similarly, Table 5 shows the corresponding drag results when both phases are power-law fluids. Here also, the effect is seen to be extremely small. This finding is qualitatively consistent with the experimental investigations of Marrucci et al. [22] and Gillapsy and Hoffer [23].

Tables 6 and 7 show the effects of the Reynolds number Re_o and the characteristic viscosity ratio k on the drag of ensembles when only the dispersed phase and when both phases behave like power-law fluids. In this case too, the rheological behaviour of the dispersed phase is seen to exert virtually no influence on the drag behaviour of the ensemble. This observation is consistent, at least qualitatively, with the approximate results of Tripathi and Chhabra [20].

Thus, in summary, the dispersed phase rheology has relatively negligible influence on the flow field in the continuous phase for single and ensembles of droplets. Therefore, their sedimentation behaviour and the rate of mass transfer in these systems is primarily governed by the non-Newtonian fluid characteristics of the continuous phase.

Finally, it is appropriate to make two comments at this juncture: firstly, the present results are based on the assumption of spherical drops (both single and in ensembles). In general, in such two phase systems, additional complications arise from drop deformation, coalescence, surface active agents, etc. which have been neglected altogether in the present study. This is justified by the fact that in Newtonian fluid systems, significant shape distortions occur beyond a critical value of the Weber number of approximately 4. This value corresponds to the Reynolds number in the range of 300–1000 depending upon the physical properties of the system. Secondly, in non-Newtonian systems, shape distortions are caused much more by visco-elasticity than that by shear-dependent viscosity [1]. Furthermore, the propensity for shape distortions diminishes with the increasing value of the viscosity ratio as the drop loses its mobility and behaves like a solid sphere. On all these counts, it is thus reasonable to neglect shape distortions over the range of conditions covered in this study.

Secondly, it is readily admitted that the power-law model fails to describe the zero shear viscosity and thus does break down near the stagnation points. On the other hand, stagnation points are singular points (of zero area) and past experience shows that in spite of this limitation, it does yield useful results for flow over a sphere. However, it is desirable to resolve this issue by carrying out a detailed study employing another more realistic viscosity model such as Cross or Carreau fluid model. As opposed to the two-parameter (m, n) power-law model used here, both the Cross and Carreau models contain three parameters (if the role of the infinite viscosity is neglected), and this will thus add another dimensionless group which combines the rheological properties with characteristic velocity and linear scale. This will thus add to the computational effort. Undoubtedly, future studies will address some of these issues. In summary, in spite of these limitations, the present results offer useful first order approximation for the estimation of drag on (or settling velocity of) single and ensembles of power-law fluid spheres in a quiescent continuous medium.

5. Conclusions

In this work, it is shown that the rheological behaviour of the dispersed phase exerts virtually no influence on the detailed flow field and drag behaviour of a single and of ensembles of fluid spheres undergoing steady translation in an immiscible quiescent liquid even for highly shear-thinning or shear-thickening conditions. On the other hand, the viscosity characteristics of the continuous phase play a significant role in governing the hydrodynamic and mass transfer characteristics in these systems. Thus, one can use the existing information to estimate the sedimentation velocity and mass transfer coefficients in these systems [7,13,18].

References

[1] R.P. Chhabra, Bubbles, Drops and Particles in Non-Newtonian Fluids, second ed., CRC Press, Boca Raton, FL, 2006, pp. 1–5, 203–204, 298–312.
[2] R. Clift, J.R. Grace, M.E. Weber, Bubbles, Drops and Particles, Academic Press, New York, 1978, pp. 125–137.
[3] G. Juncu, Int. J. Heat Fluid Flow 20 (1999) 414–421.
[4] Z.G. Feng, E.E. Michaelides, Trans. ASME J. Fluids Eng. 123 (2001) 841–849.
[5] A. Saboni, S. Alexandrova, AIChE J. 48 (2002) 2992–2994.
[6] B. Gal-Or, S. Waslo, Chem. Eng. Sci. 23 (1968) 1431–1446.
[7] N. Kishore, R.P. Chhabra, V. Eswaran, Chem. Eng. Res. Des. 84 (2006) 1180–1193.
[8] C.H. Jung, K.W. Lee, Environ. Eng. Sci. 24 (2007) 216–227.
[9] R.P. Chhabra, J.F. Richardson, Non-Newtonian Flow in the Process Industries, Butterworth–Heinemann, Oxford, UK, 1999, pp. 33–34.
[10] Y. Nakano, C. Tien, AIChE J. 16 (1970) 569–574.
[11] D. Rodrigue, J.F. Blanchet, Proceedings of the Fourth International Conference on Multiphase Flows: ICMF-2001, New Orleans, LA, May 27–June 1, 2001 (Paper#933).
[12] M. Ohta, Y. Yoshida, M. Sussman, J. Chem. Eng. Jpn. 39 (2006) 394–400.
[13] N. Kishore, R.P. Chhabra, V. Eswaran, Chem. Eng. Sci. 62 (2007) 2422–2434.
[14] D. Rodrigue, Can. J. Chem. Eng. 86 (2008) 105–109.
[15] A.B. Jarzebski, J.J. Malinowski, Chem. Eng. Sci. 41 (1986) 2569–2573.
[16] J. Zhu, W. Deng, Chem. Eng. Sci. 49 (1994) 147–150.
[17] J. Zhu, Int. J. Multiphase Flow 21 (1995) 935–940.
[18] N. Kishore, R.P. Chhabra, V. Eswaran, Chem. Eng. J. 139 (2008) 224–235.
[19] A. Tripathi, R.P. Chhabra, Arch. Appl. Mech. 62 (1992) 495–504.
[20] A. Tripathi, R.P. Chhabra, Int. J. Eng. Sci. 32 (1994) 791–803.
[21] T. Gurkan, Chem. Eng. Commun. 80 (1989) 53–67.
[22] G. Marrucci, G. Apuzzo, G. Astarita, AIChE J. 16 (1970) 538–541.
[23] P.H. Gillapsy, T.E. Hoffer, AIChE J. 29 (1983) 229–236.
[24] R.B. Bird, W.E. Stewart, E.N. Lightfoot, Transport Phenomena, 2nd ed., Wiley, New York, 2002, pp. 240–241, 844.
[25] J. Happel, AIChE J. 4 (1958) 197–201.
[26] F.H. Harlow, J.E. Welch, Phys. Fluids 8 (1965) 2182–2188.
[27] B.P. Leonard, Comput. Methods Appl. Mech. Eng. 19 (1979) 59–98.